EuCARD-HFM Project

NOTE

CERN/TE/MSC
CEA/iRFU

May 26, 2010
v 1.1

EuCARD-REP-2010-002

MPWG

EuCARD-HFM dipole model design options

Magnet Pre-design Working Group:
Mélanie Bruchon[1], Maria Durante[1], Mikko Karppinen[3], François Kircher[1], Pierre Manil[2], Attilio Milanese[3], Luc Oberli[3], Juan Carlos Perez[3], Jean-Michel Rifflet[1], Gijs de Rijk[3], Françoise Rondeaux[1], Ezio Todesco[3]

[1]*CEA Saclay/iRFU/SACM*
[2]*CEA Saclay/iRFU/SIS*
[3]*CERN/TE/MSC*

Abstract

The EuCARD-HFM task aims at realizing a 13 T dipole magnet with an aperture of 100 mm, which is a challenging step towards very high field accelerator magnets. This dipole, utilizing Nb_3Sn superconductor, will be used in the Fresca test facility at CERN. A preliminary design study has compared two possible design layouts for the EuCARD-HFM magnet: the cos-θ and the block. This report summarizes the conclusions of this study and justifies, on the base of quantitative and qualitative arguments, our decision to pursue the detailed design with the block layout.

Content

Introduction

Magnets with Nb_3Sn conductor are needed to upgrade existing accelerators in Europe such as the LHC, and to prepare for new projects on a longer timescale. Their high current density properties in high fields and large temperature margin will be needed to meet the field and gradient requirements and to withstand the heating due to the radiation in these new and upgraded machines [1]. Nb_3Sn is today the right candidate to meet those objectives, because of its superconducting properties and its industrial availability. However, this material is brittle and strain-sensitive after reaction, so its practical application remains challenging.

On the very long term, further upgrades could require dipole magnets with a field of around 20 Tesla (T). These accelerator magnets are beyond the possibilities offered by using Nb_3Sn conductors alone. A possibility is to combine an outer Nb_3Sn coil with an inner coil of High Critical Temperature (HTS) conductor, both contributing to the field.

The European project EuCARD aims at addressing these technological challenges.

The goal of its task 7.3 (High Field Magnet) is to design and build a dipole magnet capable to reach 13 T at 4.2 K. It should be representative of accelerator magnets and could approach 15 T at 1.9 K. The specified aperture of 100 mm puts the EuCARD-HFM dipole in an unexplored domain, justifying careful developments. In addition, the dipole will be used to upgrade the Fresca test facility at CERN, in the aim of meeting the strong need to qualify conductor at higher fields. The delivery of the magnet is scheduled by mid-2013. This rather short delay leads to reduce the technical risks as most as possible.

The task 3 has been divided into three working groups:

- Specification (SWG),
- Cable Design (CDWG),
- Magnet Pre-design (MPWG).

This study is in the framework of the MPWG, gathering people from CERN and CEA Saclay. The specification and the cable features are considered as inputs.

After setting-up the collaborative work and producing preliminary estimates, we have focused on two layouts for the dipole magnet: cos-θ and block. These two types of configurations have already been used with less demanding field and aperture in different magnet designs around the world, for Nb-Ti as well as Nb_3Sn. Due to our time constraints and available resources, we now need to choose one solution before launching the detailed study.

The aim of this report is to list and to discuss the reasons behind our choice. A baseline 2D magneto-mechanical analysis compares quantitatively both layouts. Then, the qualitative arguments that have driven our decision are listed. Among them, the possibility to make the ends with the block layout, for which less experience is available than for the cos-Θ, has been experimentally verified in a representative case.

1. Inputs

1.1 Scope of the study

EuCARD requires a magnetic field of 13 T in a 100 mm-diameter bore. The specified dipole length is 1.5 m.

This meets the Fresca cable test facility upgrade requirements, that also impose a field homogeneity of 2% at 2/3 of the bore aperture over a sample length. Operation in the facility involves some additional constraints in terms of space, power supply limits and stray field. The input constraints imposed to the EuCARD-HFM dipole are listed as defined today in § 1.2.

It is envisaged to push the central field up to 15 T while working with superfluid helium around 1.9 K. This additional goal is kept in mind along the study but will not determine our decisions.

Even if this study is focused on achieving the target field and aperture, the accelerator magnet requirements are kept in mind. For instance, despite the lower expected field quality, the following analysis will take into account the possibility to achieve accelerator-compatible homogeneity. In the same way, no challenging constraint is given on the field time-dependence, although this is an important parameter for accelerators.

The complexity of the cable development and production imposes long procurement delays and high costs. The amount of conductor available in two years will be limited; therefore, the number of possible attempts will be limited as well. That is why we are forced at the moment to focus on one option. The tight schedule and available resources impose that the decision on the layout type is made now.

The necessity to reduce the technical risk has driven us to concentrate on two possible layouts: cos-θ and block. Solutions requiring more development, such as hybrid or graded coils, have been discarded. Indeed, these options would suppose longer development phases with less flexibility on the conductor use.

It has been decided to use epoxy-impregnated glass fibre insulation as developed during the CARE-NED project [2], even if this solution is not satisfactory for the high level of radiations expected in future accelerator magnets. A separate task focuses in parallel on enhanced insulation schemes.

The dipole design has interactions with the thermal studies (helium circulation in the structure, shielding) and the HTS insert (assembly, coupling, failure). This introduces additional interfaces and constraints that will be addressed during the detailed study, but that do not determine the layout choice. In particular, the mechanical structure of the insert should be removable, self-supporting and fixed longitudinally. The eventuality of an interference with the dipole will be studied by a specific working group.

1.2 Specifications and constraints

The following table summarizes the EuCARD-HFM dipole inputs, as defined by the SWG [3]. The different sources may lead to some redundancies. Additionally there are implicit cost constraints.

Parameter name		Symbol	Unit	Value	Source[1]	Remarks
MAGNETIC SPECIFICATIONS						
Central field		B_0	T	13	EuCARD/FRESCA	at 4.2 K
Clear bore aperture		Φ_b	mm	100	EuCARD/FRESCA/HTS	Interface with HTS insert
Magnetic field multipoles[2]		b_3, $b_{5...}$	/	≤ 10	EuCARD	at 2/3 Φ_b
Magnetic field homogeneity		$\Delta B/B_0$	%	2	FRESCA/De Rijk	at 2/3 Φ_b over the straight part
Stray magnetic field		B_{out}	T	≤ 0.2	CERN safety rule	at personnel location
Operational temperature		T	K	1.9 to 4.2	Test station	
Current		I	kA	≤ 20	Test station	
DIMENSIONAL CONSTRAINTS						
Magnet length		L_{pole}	mm	1500	EuCARD	Coil end-to-end
Magnet pole width		w_{pole}	mm	≤ 350	Furnace	
Magnet pole height		h_{pole}	mm	≤ 200	Furnace	
Magnet straight section length		L_{ss}	mm	≥ 800	FRESCA	
Cold mass outer diameter		Φ_{tot}	mm	≤ 1300	Test station	
Cold mass length		L_{tot}	mm	≤ 2500	Test station	
CONDUCTOR FEATURES						
Number of strands		N_{str}	/	40	CDWG	
Keystone angle		α	°	0	CDWG	
Strand diameter		Φ_{str}	mm	1.00	CDWG	± 0.1 mm
Cu / non Cu rate		$r_{Cu/nCu}$	/	1.25	CDWG	
Cable width		w_{cbl}	mm	21.4	CDWG	
Cable thickness at 50 MPa		t_{cbl}	mm	1.82	CDWG	
Transposition pitch		p	mm	120	CDWG/Oberli	Left-handed screw thread direction
Critical current with field normal to broad face	at 15 T	$I_{ss,\ 15T}$	A	15710	CDWG	at 4.2 K
	at 12 T	$I_{ss,\ 12T}$	A	31420	CDWG	at 4.2 K
Minimum critical current of extracted strand	at 15 T	$I_{ss,min,\ 15T}$	A	393	CDWG	at 4.2 K
	at 12 T	$I_{ss,min\ 15T}$	A	786	CDWG	at 4.2 K
INSULATION FEATURES						
Insulation type		/	/	Fibreglass + epoxy	CDWG/CARE-NED	Incompatible with high radiation levels
Insulation thickness		t_{ins}	mm	0.2	CDWG/CARE-NED	Per conductor face

Tab. 1.2.1. EuCARD-HFM dipole specifications and constraints

[1] Sources: EuCARD = EuCARD project contractual requirements [4]; FRESCA = FRESCA2 specification; Test station = existing Fresca test station constraints; CDWG = Cable Design Working Group; Oberli = communication from Luc Oberli (MPWG Meeting 05, CERN, 25 Feb. 2010); De Rijk = email from Gijs de Rijk to Pierre Manil (10 May 2010); CARE-NED = [2].

[2] The magnetic field multipoles are computed at 2/3 of the bore using the reference value of 10^4 for the main dipolar component.

1.3 Baseline conductor

The EuCARD-HFM cable was designed in such a way that the large aperture dipole can reach a bore field up to 15 T at 4.2 K. Several constraints have been taken into consideration to define the parameters of the EuCARD-HFM cable. First of all, the maximum number of strands in the cable has been fixed to 40 in order to be able to fabricate the cable with the cabling machine installed at CERN. Secondly, the maximum operational current of the dipole has been limited to 20 kA to be compatible with existing power convertors and current leads in the test station.

1.3.1 Strand

According to the results obtained by industry in the program launched by CERN in the framework of the CARE-NED project to develop a Nb_3Sn strand with a diameter of 1.25 mm and with 50 µm diameter filaments, the critical current density of the Nb_3Sn strand achievable for the EuCARD-HFM program has been fixed to a minimum value of 1250 A/mm^2 at 15 T and 4.2 K. The strand diameter to be used for the EuCARD-HFM cable has been fixed at 1 mm instead of 1.25 mm as in the CARE-NED project for several reasons. The main reason for the choice of the 1 mm diameter strand is to improve the magneto-thermal stability with respect to the 1.25 mm diameter strand. This choice is a compromise between the request to have a transport current for the cable high enough to reach a central field up to 15 T in the dipole and to avoid self-field instabilities in the low field regions of the dipole.

In the following analysis, the critical current surface of the strand is modelled using the Summers I critical current fit available in ROXIE [5], as:

$$J_c(B,T) = \frac{C}{\sqrt{B}}\left(1-\frac{B}{B_{c2}(T)}\right)^2 \cdot \left[1-\left(\frac{T}{T_{c0}}\right)^2\right]^2,$$

$$B_{c2}(T) = B_{c20}\left[1-\left(\frac{T}{T_{c0}}\right)^2\right]\left\{1-0.31\left(\frac{T}{T_{c0}}\right)^2\left[1-1.77\ln\left(\frac{T}{T_{c0}}\right)\right]\right\},$$

where T is the temperature and B the magnetic field. Fitting this curve with 2500 A/mm^2 at 12 T, 4.2 K and 1250 A/mm^2 at 15 T, 4.2 K, returns the following parameters for the virgin strand: T_{c0} = 18 K, B_{c20} = 28 T and $C = 35 \cdot 10^9$ A/m^2. Factoring in a 10% degradation due to cabling returns the J_c fit of Fig. 1.3.1.

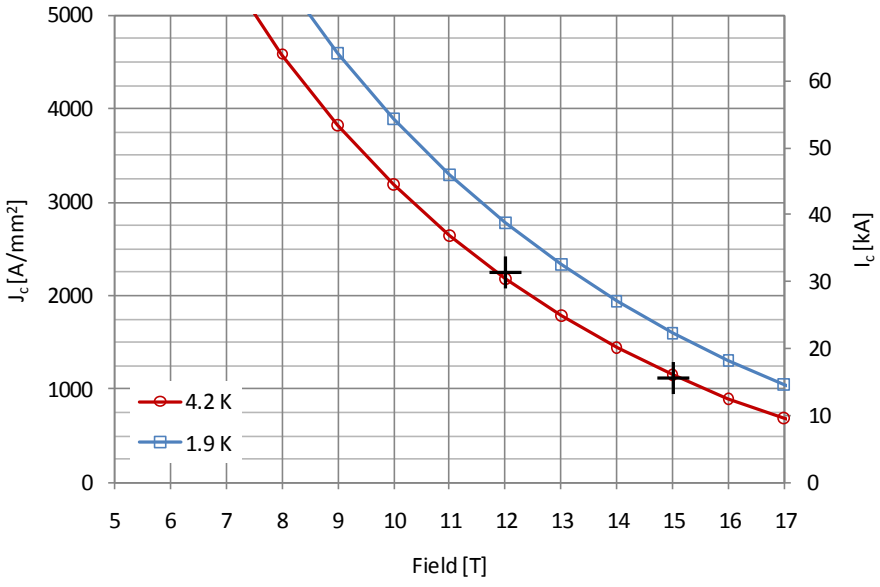

Fig. 1.3.1. Critical surface fit of extracted strand, including 10% degradation due to cabling

1.3.2 Cable

The main characteristics of the cable for the EuCARD-HFM program are reported in Tab. 1.2.1. The cable is a Rutherford-type cable with no keystone angle, consisting of 40 strands. The minimum critical current at 4.2 K is 15710 A at 15 T (31420 A at 12 T). The critical current in the finished cable is defined as the current measured at an electrical field of 10 μV/m. The cable critical current assume a cable degradation of 10 %. The cable transposition pitch has been fixed to a value of 120 mm after cabling tests performed with copper wires showing that the cables do not have a good mechanical stability for transposition pitches greater than this value.

1.4 Other inputs

In the following, it is assumed a distance of 10 mm between the clear bore and the coil to be used by the structure (mechanical support and cryogenic system) and the bore tube.

2. Historical background

To give a full account of superconducting dipoles designed, built and tested in the last 30 years is not within the scope of this report. The exercise is easier if we limit ourselves to Nb_3Sn magnets, but also in this case a comprehensive list would be too long in this context. Here we present:

- some information about apertures and fields attained in selected Nb-Ti / Nb_3Sn dipoles,
- some details about D20, a Nb_3Sn cos-θ dipole,
- some details about HD2, a Nb_3Sn block dipole.

This will better situate the design goals of the magnet under development with respect to what has already been achieved, while providing references to cos-θ and block layouts already explored in other designs.

2.1 Apertures and fields attained in selected superconducting dipoles

A plot of design short sample field versus bore diameter is reported in Fig. 2.1.1 for selected superconducting magnets. For Nb-Ti ones, preference has been given to accelerator dipoles. The data has been retrieved from [6] and [7]. The data is normalized in the sense that the conductor properties used to compute the short sample field are kept constant across the families of Nb-Ti or Nb_3Sn magnets. Therefore, the improvement in performance of the superconducting material over the years is taken out of the comparison.

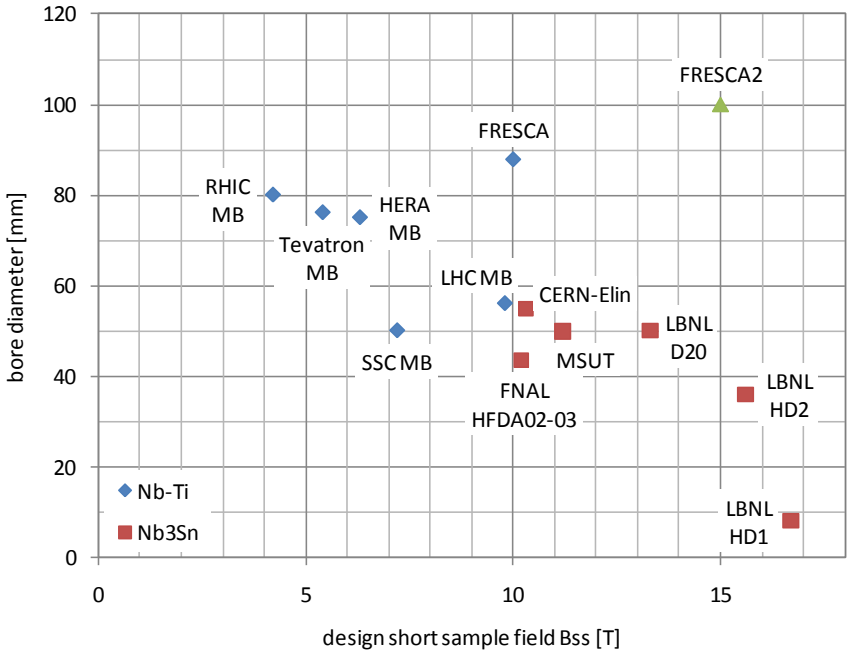

Fig. 2.1.1. Map of selected dipoles: design short sample field versus bore diameter

Nb_3Sn becomes a necessary option when short sample fields above 10 T need to be reached. To this day, HD1 owns the field record for dipoles (16 T at ~95% of its short sample limit) which is however attained in a rather small bore (less than 10 mm). Indeed, HD1 is the first dipole in a series conceived to push the conductor to its physical limit, while gradually increasing the aperture. The EuCARD-HFM marker refers to the dipole whose pre-design is considered in this report. For that, a short sample field around 15 T is envisaged, so that specified operation field of 13 T at 4.2 K will involve a reasonable margin.

2.2 The dipoles D20 and HD2

From the data presented in Fig. 2.1.1, D20 and HD2 can be considered two close predecessors of the EuCARD-HFM dipole to be developed. Both dipoles come from the Lawrence Berkeley National Laboratory (LBNL) Superconducting Magnet Group and will be briefly described next.

D20 [8]-[9] is a 50 mm bore, 1-m long dipole intended for R&D on high field magnets. It was developed in the 1990's and it was used in a test facility for critical current measurements. The cross section of the coil is shown in Fig. 2.2.1, while its training history is shown in Fig. 2.2.2.

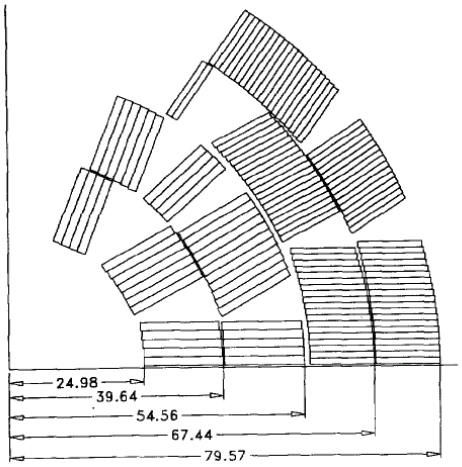

Fig. 2.2.1. Cross section of D20 (a quarter shown)

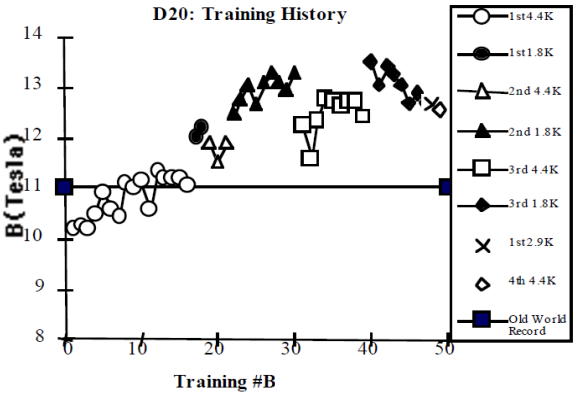

Fig. 2.2.2. Training history of D20

A graded cos-θ design was used, with four layers wound with two different cables. Both the inner and outer layers cables are rectangular, as fabrication of key-stoned ones resulted in unacceptably large critical current degradation [10]. The short sample field at 4.2 K was around 14 T and the dipole attained about 90% of its short sample limit after 30 training quenches.

HD2 [11] is a 36 mm bore, 1-m long dipole, that constitutes the next step after HD1 (a magnet with flat racetrack coils) towards block-type accelerator quality dipoles. It is a rather recent magnet, whose first tests have been presented in 2008. The cross section of the coil – together with part of the support structure – is shown in Fig. 2.2.3; the training history is plotted in Fig. 2.2.4.

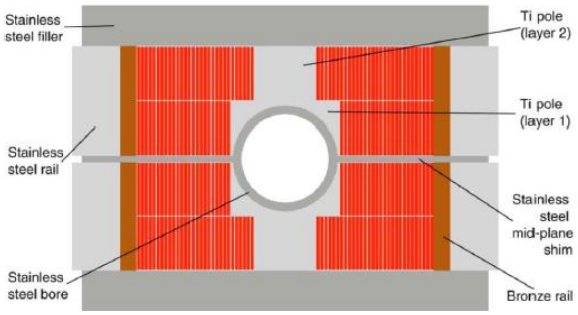

Fig. 2.2.3. Cross section of HD2

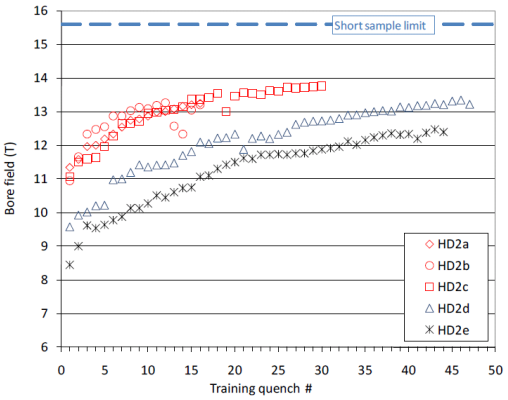

Fig. 2.2.4. Training history of HD2

The design is based on a block layout for the coils. The support structure involves the use of bladder and keys and a shrinking aluminum alloy cylinder to provide pre-stress at warm / cold. The ends of the coils are flared, with a hard-way bend, a 10° ramp and an easy-way bend. The training history shows that the magnet reached 13.8 T corresponding to about 90% of its short sample limit after 30 quenches. The group at LBNL is currently working on HD3, a modified version of HD2 with a 43 mm bore and modifications aimed at improving the quench performance of the magnet [12].

3. Analytical estimates

Before embarking on a detailed magnetic design of the cross section, the amount of conductor needed can be estimated using the analytical approach of [6]. In this method, it is assumed that the coil is a sector coil, as shown in Fig. 3.1. In particular, a [0-60°] layout and a [0-48, 60-72°] layout are used: the latter has a better field quality that is traded for some field strength.

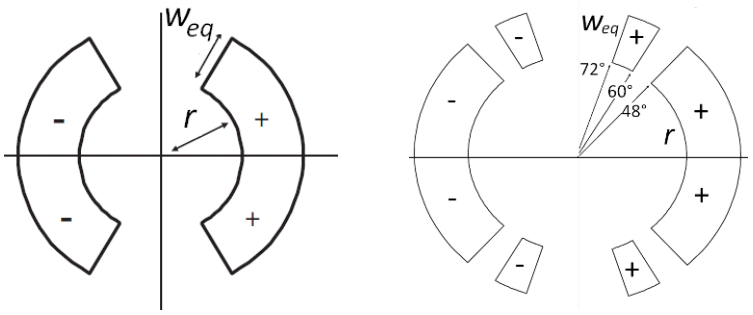

Fig. 3.1. Schematic layout of a 60° sector coil (left) and a [0-48, 60-72°] sector coil (right) for a dipole of aperture radius r and coil width w_{eq}

The radius r in this analysis is set to 60 mm because it is envisaged that some material in between the coil and the bore is needed to:

- hold the necessary pre-stress (cf. §1.4),
- guarantee a sound interface with the HTS dipole insert [13].

The ratio λ between peak field on the coil and central field scales with the aspect ratio as

$$\lambda(w,r) = 1 + a\frac{r}{w_{eq}},$$

where a = 0.06. This hyperbolic fit is obtained for sector coils and is adequate for cos-θ dipoles. In the case of a block design, λ is likely to be higher, for the same radius and equivalent width.

The short sample field at 4.2 K, $B_{ss,\,4.2\,K}$, is obtained from

$$B_{ss,4.2K} = \frac{\kappa c \gamma_0 w_{eq}}{2}\left(\sqrt{\frac{4b}{\kappa c \lambda \gamma_0 w_{eq}} + 1} - 1\right)$$ with the parameters:

- filling factor κ = 0.289 (from cable specification, § 1.3),
- c = 3375 A/mm^2, b = 20 T for the hyperbolic critical surface fit at 4.2 K,
- c = 3625 A/mm^2, b = 21.5 T for the fit at 1.9 K,
- γ_0 = 6.928·10^{-7} Tm/A for the [0-60°] sector coil and γ_0 = 6.625·10^{-7} Tm/A for the [0-48, 60-72°] one.

Tab. 3.2 contains a parametric analysis performed varying the amount of conductor. The width w_{eq} of the sector coil is computed from the number of turns of cable per pole. The short sample fields are reported at 4.2 K and 1.9 K for the two sector geometries considered.

From this analysis, a tentative number of 156 turns of cable per pole has been selected. This is based on the following arguments:

- $B_{ss,\,1.9\,K}$ for a [0-48, 60-72°] sector coil dipole without iron is in the 15 T region for 150-160 turns,
- the iron is likely to increase this value by about 5% [6],
- the peak field over central field ratio λ may be less favorable than assumed, thus equaling out the contribution of the iron.

The equivalent width w_{eq} for 156 turns is w_{eq} = 74.2 mm. For a cos-θ configuration, and assuming that about 15% is used up for wedges, a physical width of w = 85.3 mm is needed. Thus, in a cos-θ layout and using a cable about 21 mm wide, four layers are needed.

The following comparative study considers the number of turns equal to 156.

Number of turns (per pole) [/]	w_{eq} [mm]	λ [/]	[0-60°] sector coil		[0-48, 60-72°] sector coil	
			$B_{ss,\ 4.2\ K}$ [T]	$B_{ss,\ 1.9\ K}$ [T]	$B_{ss,\ 4.2\ K}$ [T]	$B_{ss,\ 1.9\ K}$ [T]
70	40.3	1.09	12.6	13.5	12.0	12.9
80	44.9	1.08	13.0	13.9	12.4	13.3
90	49.2	1.07	13.3	14.3	12.7	13.7
100	53.3	1.07	13.6	14.6	13.0	14.0
110	57.3	1.06	13.9	14.9	13.2	14.2
120	61.2	1.06	14.1	15.1	13.5	14.5
130	65.0	1.06	14.3	15.4	13.7	14.7
140	68.6	1.05	14.5	15.6	13.8	14.9
150	72.2	1.05	14.6	15.7	14.0	15.1
156	74.2	1.05	14.7	15.8	14.1	15.2
160	75.6	1.05	14.8	15.9	14.2	15.2
170	79.0	1.05	14.9	16.1	14.3	15.4
180	82.3	1.04	15.1	16.2	14.4	15.5
190	85.5	1.04	15.2	16.3	14.5	15.6
200	88.6	1.04	15.3	16.4	14.6	15.7

Tab. 3.2. Analytical estimates of short sample fields based on sector coils (without iron)

4. Quantitative comparison

4.1 Cos-θ layout

4.1.1 Magnetic performance

According to the analysis of the previous section, the 156 turns of 21.4 mm-wide Rutherford cable in a cos-θ configuration need to be arranged in four layers, approaching as much as possible the theoretical w_{eq} value of 74 mm. Among the many ways of doing so, a first baseline layout has been obtained – without considering the effect of the iron – as follows:

- the radius of the winding mandrel of the innermost layer has been fixed to 60 mm (§ 1.4),
- a radial distance of 0.5 mm between the insulated cables in adjacent layers has been used,
- a mid-plane shim of 2 × 0.2 mm thickness has been imposed,
- a 3 + 3 + 3 + 3 configuration, with three blocks per layer, has been adopted (an alternative would have been, for example, a 4 + 4 + 2 + 2 scheme),
- the angles have been set as to position the cables as radially as possible, to ease winding of the ends,
- the number of conductors per block and the overall geometry have been chosen as to have good field quality in the bore, i.e., the multipoles b_3, b_5 and b_7 have been minimized.

The resulting cross section is described, using the notation and units of ROXIE [5], in Tab. 4.1.1. The numbering of the layers starts with the inner ones and proceeds outwards.

Layer	Block	N_{cbl}	R	ϕ	α
1	1	9	60.0	0.2	0.0
	2	12	60.0	21.5	34.5
	3	7	60.0	56.1	62.1
2	4	11	82.3	0.1	0.0
	5	18	82.3	19.0	32.5
	6	8	82.3	56.9	63.9
3	7	15	104.6	0.1	0.0
	8	18	104.6	20.0	31.0
	9	10	104.6	49.3	53.6
4	10	16	126.9	0.1	0.0
	11	16	126.9	17.3	25.3
	12	16	126.9	34.5	42.7

Tab. 4.1.1. Baseline cos-θ configuration

This cross section is presented in Fig. 4.1.2, where the field in the coil for a bore field of 13 T is shown, and relevant magnetic figures are reported.

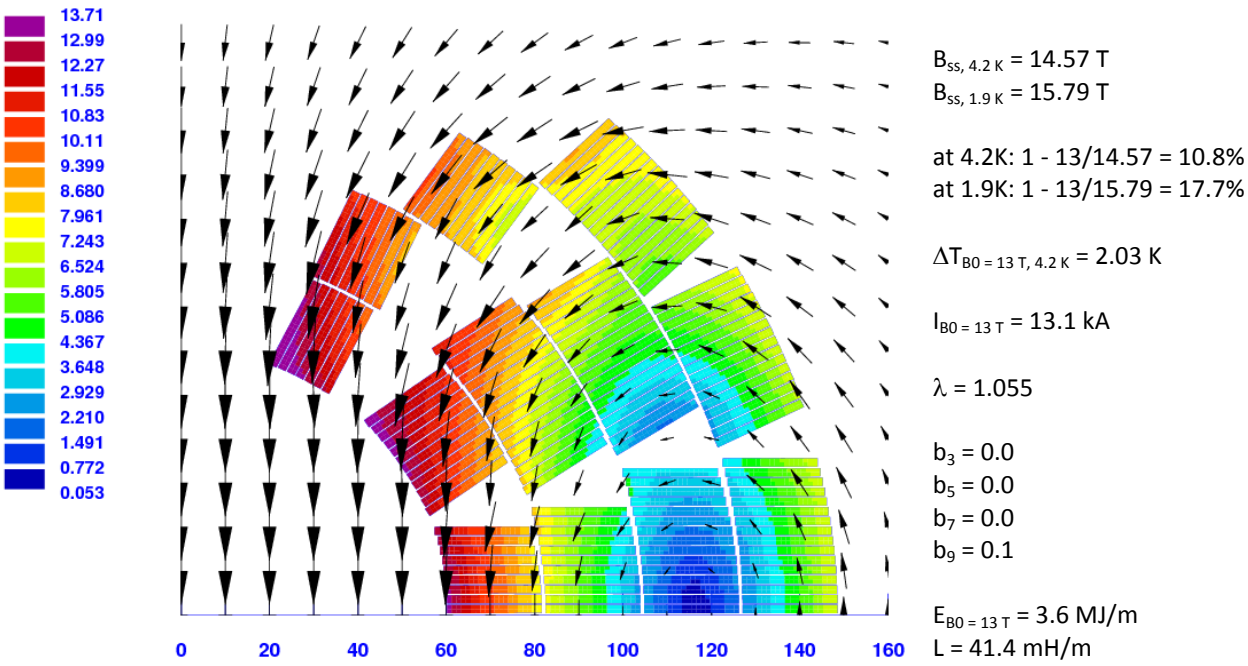

Fig. 4.1.2. Baseline cos-θ cross-section (a quarter shown).
The field in the coil is computed for a 13 T bore field.

The effect of the iron is to decrease the current in the coils needed to reach 13 T in the bore. Therefore, it is likely that the Lorentz forces on the conductors will be lower when iron is considered. Here, since the geometry of the magnetic yoke and/or pads has not been designed yet, the method of mirror images is used. The iron is assumed to provide a 5% increase on $B_{ss,\ 1.9\ K}$. A suitable radius R for a circular mirror (with relative permeability μ_r = 1000) can then be found. In this case, such a radius is equal to R = 225 mm. With this approach, the current needed to have 13 T in the bore decreases from 13.1 kA to 10.7 kA. A plot of the forces with and without iron is shown in Fig. 4.1.3.

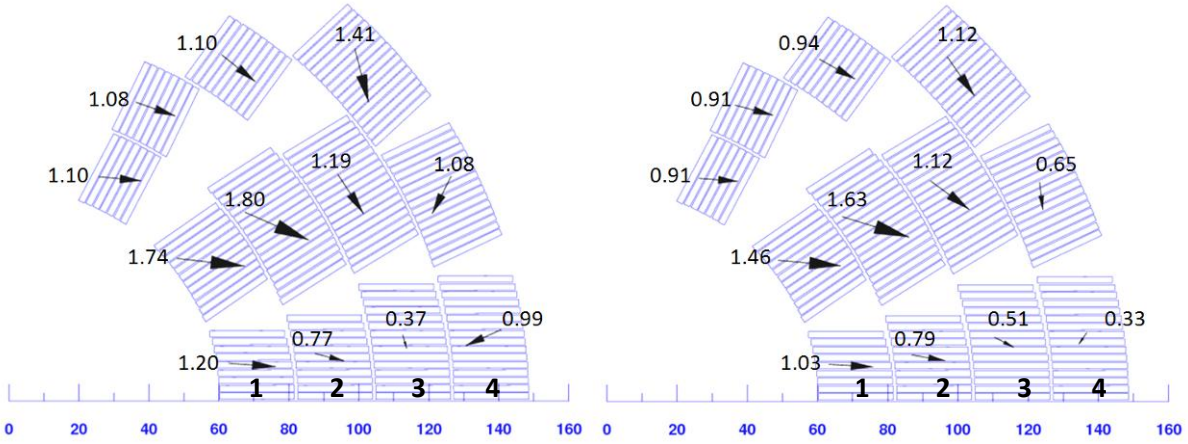

Fig. 4.1.3. Forces in the cos-θ layout without (left) and with (right) iron, for a 13 T bore field.
The values indicate the magnitudes of the forces in MN/m. Layer numbers are indicated.

4.1.2 Mechanical stress estimation

Next, an evaluation of the stresses on the coil due to the Lorentz forces follows. A first estimation of the azimuthal stresses on the mid-plane can be obtained adding up the azimuthal components of the forces and then dividing by the width of the cable. The result of this estimation is reported in Tab. 4.1.4.

Layer	1	2	3	4
Mean azimuthal stress [MPa]	110	131	122	101

Tab. 4.1.4. Mean azimuthal stresses on the cos-θ layout, computed directly from the forces. The values refer to the layout without iron, powered as to reach 13 T in the bore.

An ANSYS [14] model of the coil and wedges has been set up, with the following assumptions:

- The coils and wedges are represented by PLANE42 elements, in plane strain.
- Isotropic material properties are used, with Young modulus E and Poisson ratio ν as E_{coil} = 42 GPa, E_{wedge} = 110 GPa, $\nu_{coil} = \nu_{wedge}$ = 0.3. These are the cryogenic properties of impregnated Nb_3Sn cable and copper alloy, from [15]. The thermal stresses are not considered in this baseline computation.
- The various interfaces are modeled with TARGE169 / CONTA172 contact elements pairs, with friction coefficients μ as follows:
  - between 1st and 2nd layer, $\mu_{1\text{-}2}$,
  - between 2nd and 3rd layer, $\mu_{2\text{-}3}$,
  - between 3rd and 4th layer, $\mu_{3\text{-}4}$,
  - between 4th layer and outer circular arc, $\mu_{4\text{-}out}$,
  - between conductors and mid-plane, μ_{mid}.
- Rigid boundary conditions on the mid-plane and on the outer circular arc are imposed.

Figure 4.1.5 shows the azimuthal component of the stresses in two extreme cases, where all the friction coefficients are set to 0 (pure sliding) and when they are set to 1000 (almost pure sticking). These extreme cases, that help understand the role of friction, are not to be considered directly for the layouts comparison. These stresses arise from the Lorentz forces for a bore field of 13 T; the forces are computed strand by strand in ROXIE.

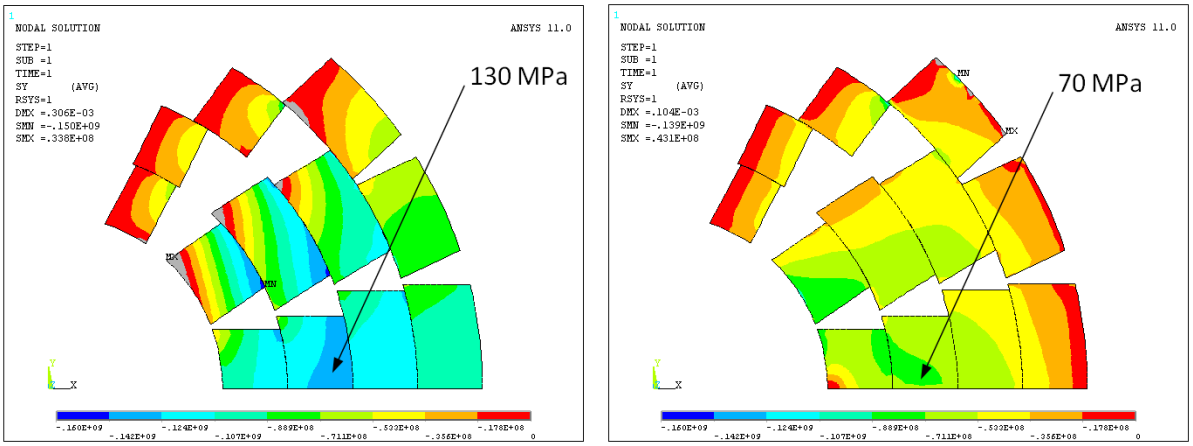

Fig. 4.1.5. Azimuthal stress distribution for the **extreme cases** μ = 0 (left) and μ = 1000 (right) models, for a 13 T bore field.

In the case with μ = 1000, the peak azimuthal stress on the mid-plane is sensibly lower than for the μ = 0 model. In fact, when the layers are able to transmit tangential stresses between them, the effect is that the Lorentz forces are better averaged and the peaks are lowered. A good impregnation could be beneficial in this regard, although winding, curing and potting four layers at once could be particularly challenging.

If the layers are impregnated in pairs, a more physical model could involve the following friction coefficients: $\mu_{1\text{-}2}$ = 1000, $\mu_{2\text{-}3}$ = 0.2, $\mu_{3\text{-}4}$ = 1000, $\mu_{4\text{-}out}$ = 0.2, μ_{mid} = 0.2. The resulting plots of the azimuthal and Von Mises stresses are reported in Fig. 4.1.6.

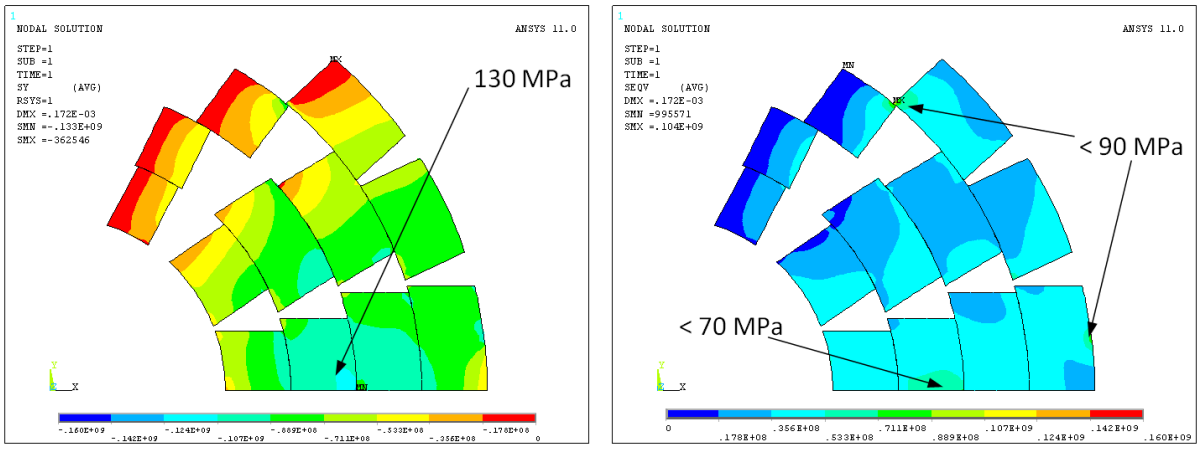

Fig. 4.1.6. Case with $\mu_{1\text{-}2}$ = 1000, $\mu_{2\text{-}3}$ = 0.2, $\mu_{3\text{-}4}$ = 1000, $\mu_{4\text{-}out}$ = 0.2, μ_{mid} = 0.2, for a 13 T bore field. Azimuthal stresses are plotted on the left, while Von Mises ones are on the right.

Based on these analyses, the peak azimuthal stress on the conductor coming from Lorentz forces is estimated to be around 130 MPa, for a 13 T field in the model.

A more precise finite element model for the stresses should – among other things – consider:

- the magnetic effect of the iron,
- the overall support structure, with the stiffness and the differential thermal contractions of the various components,
- the applied pre-stress.

4.2 Baseline block layout

4.2.1 Magnetic performance

A baseline block design – without considering first the effect of the iron – has been obtained using similar constraints as for the cos-θ configuration. In particular:

- 156 turns of cable (per pole) have been used,
- for the blocks closer to the mid-plane, the first conductors are placed at a horizontal distance equal to 60 mm from the centre (cf. §1.4),
- the blocks farther away from the mid-plane are at a 55 mm vertical coordinate, as to be clear of the bore with a reasonable margin for cryogenics and structure,
- a distance of 0.5 mm between the insulated cables in adjacent layers has been introduced,
- a 1 + 1 + 1 + 1 configuration, with four layers without additional wedges, has been adopted, grouping the layers in pairs (double-pancake configuration),
- the number of conductors per block, as well as the horizontal and vertical positions, have been set as to have good field quality, i.e., the first multipoles have been minimized,

The resulting cross section is described, using the notation and units of ROXIE [5], in Tab. 4.2.1. The numbering of the layers starts with the one closer to the mid-plane and proceeds vertically.

Block	N_{cbl}	X	Y	α
1	41	151.02	5.06	90
2	41	151.02	27.36	90
3	37	116.13	55.0	90
4	37	116.13	77.3	90

Tab. 4.2.1. Baseline block configuration

This cross section is presented in Fig. 4.2.2, where the field in the coil for a central field of 13 T is shown, and relevant basic magnetic figures are reported.

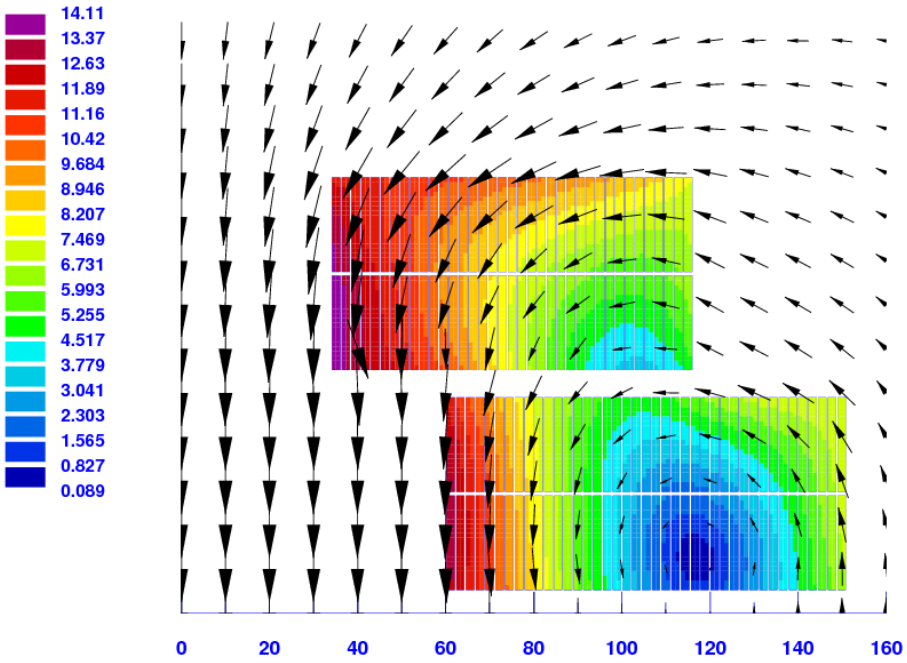

Fig. 4.2.2. Baseline block cross section (a quarter shown).
The field in the coil is computed for a 13 T bore field.

The contribution to the central field is given at 62% from the blocks closer to the mid-plane (blocks 1-2), and at 38% from the other ones (blocks 3-4)

The short sample fields at 1.9 K using only blocks 1-2 is 12.2 T, while using only blocks 3-4 it is 8.8 T.

This design involves a peak field / central field ratio λ higher than the one expected from a sector coil of similar r and w_{eq}. However, this ratio can be brought back to around 1.05 (with a corresponding increase in short sample field) by making the field quality constraints looser. Keeping a similar 1 + 1 + 1 + 1 topology, with pair-wise coupled blocks, the "maximum strength" configuration can be attained by moving the lower blocks closer to the mid-plane, and by shifting the two upper ones outward. The gain in short sample is about 0.4 – 0.5 T, with a sextupole around 100 units.

For this layout, the support structure may be conceptually similar, for example, to the one of HD2 [11], with a bladder and key system to provide part of the pre-stress at room temperature, and a surrounding shell to provide the rest at cold. Therefore, a tentative geometry for vertical / horizontal iron pads and yoke have been used to estimate the influence of the iron, including saturation. The magnetic properties of the material of the LHC MB yokes have been used [16]. Figure 4.2.3 shows a sketch of the magnetic iron elements surrounding the coils.

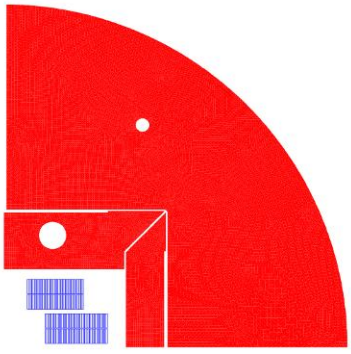

Fig. 4.2.3. Baseline block layout with surrounding iron pads and yoke (a quarter shown).

Such an iron decreases the current needed to achieve 13 T in the bore from 13.4 kA to 11.1 kA. The short sample field at 4.2 K goes from 14.2 T to 14.8 T, while the one at 1.9 K increase from 15.4 T to 15.9 T. A further considerable increase in short sample – of the order of 0.8 T [17] – could be achieved by winding the two upper blocks on an iron pole. The magnetic drawback of this solution would be the highly nonlinear distortion of the field in the bore as a function of the current. A plot of the Lorentz forces with and without iron (pads & yoke) is shown in Fig. 4.2.4.

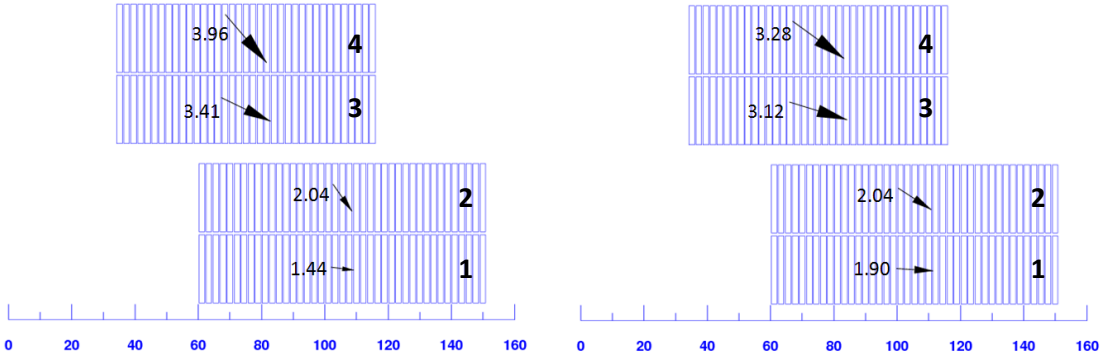

Fig. 4.2.4. Forces in the block layout without (left) and with (right) iron, for a 13 T bore field. The values indicate the magnitudes of the forces in MN/m. Block numbers are indicated.

4.2.2 Mechanical stress estimation

Next, an estimation of the stresses on the coils due to the Lorentz forces follows. A first guess of the horizontal stresses on the conductors further away from the centre can be obtained dividing the horizontal components of the forces by the width of the cable, block by block. The result of this estimation is reported in Tab. 4.2.5. These values can be considered only indicative, as – for example – they do not consider the build-up and reversal of forces due to the change of direction of the magnetic field in the lower blocks. Furthermore, this estimate assumes perfect sliding between the various interfaces.

Block	1	2	3	4
Mean horizontal stress [MPa]	65	54	141	119

Tab. 4.2.5. Mean horizontal stresses on the outer conductors for the block layout, computed directly from the forces. The values refer to an ironless layout, powered as to reach 13 T in the bore.

An ANSYS [14] model of the four blocks, with an in between wedge element to transfer the forces, has been set up, with the following assumptions:

- The coils and wedge are represented by PLANE42 elements, in plane strain.
- Isotropic material properties are used, with Young modulus E and Poisson ratio ν as E_{coil} = 42 GPa, E_{wedge} = 110 GPa, $\nu_{coil} = \nu_{wedge}$ = 0.3. These are the cryogenic properties of impregnated Nb_3Sn cable and copper alloy, from [15]. The thermal stresses are not considered in this baseline computation.
- The various interfaces are modeled with TARGE169 / CONTA172 contact elements pairs, with friction coefficients μ as follows:
  - between 1st and 2nd layer, $\mu_{1\text{-}2}$,
  - between 3rd and 4th layer, $\mu_{3\text{-}4}$,
  - between the coils layer and the wedge, as well as with the outer surfaces, μ_{other}.
- Rigid boundary conditions on the mid-plane and on the rightmost surface are imposed.

Figure 4.2.6 shows the horizontal component of the stresses in two extreme cases, where all the friction coefficients are set to 0 (pure sliding) and when they are set to 1000 (almost pure sticking).

These stresses arise from the Lorentz forces for a bore field of 13 T; the forces are computed strand by strand in ROXIE, without including the iron.

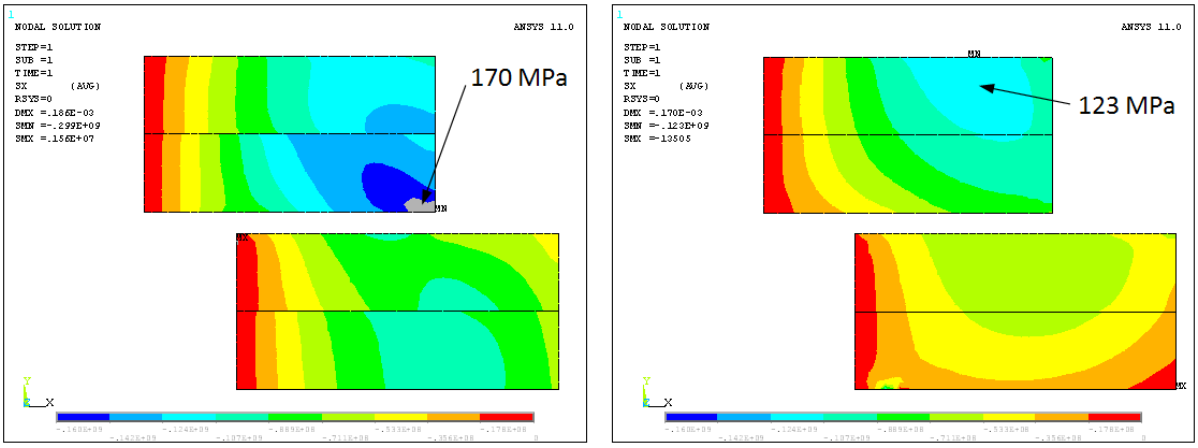

Fig. 4.2.6. Horizontal stress distribution for the **extreme cases** μ = 0 (left) and μ = 1000 (right), for a 13 T bore field.

When the horizontal Lorentz forces are shared by the blocks (this is simulated by a high friction coefficient) the peak horizontal stress is considerably lowered. Furthermore, in both cases the build-up of the forces results in concentration of stresses in regions where the magnetic field is lower. This could be beneficial in the case of degradation of the critical current of the superconductor due to mechanical stress.

If the layers are impregnated in pairs (double-pancakes), a more physical simulation could involve the following friction coefficients: $\mu_{1\text{-}2} = 1000$, $\mu_{3\text{-}4} = 1000$, $\mu_{other} = 0.2$. The resulting plots of the horizontal and Von Mises stresses are reported in Fig. 4.2.7.

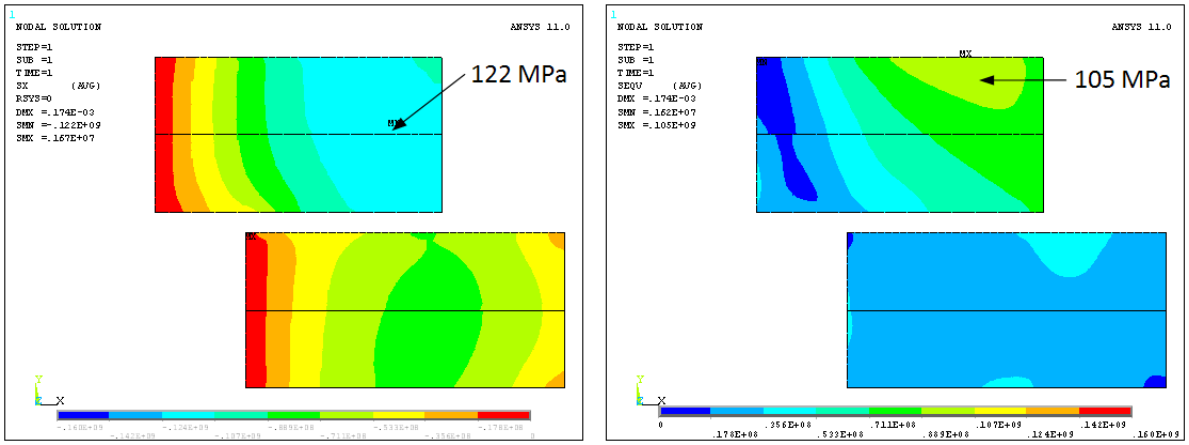

Fig. 4.2.7. Case with $\mu_{1\text{-}2} = 1000$, $\mu_{3\text{-}4} = 1000$, $\mu_{other} = 0.2$, for a 13 T bore field.
Horizontal stresses are plotted on the left, while Von Mises ones are on the right.

Based on these analyses, the peak azimuthal stress on the conductor coming from Lorentz forces is estimated to be around 125 MPa, for a 13 T field in the model.

As for the cos-θ layout, a more precise finite element model for the stresses should – among other things – consider:

- the magnetic effect of the iron,
- the overall support structure, with the stiffnesses and differential contractions of the various components,
- the applied pre-stress.

4.3 Quantitative comparison summary

Parameter name	Symbol	Unit	Cos-θ	Block
MAGNETIC PARAMETERS				
Central field	B_0	T	13	13
Short sample field, at 4.2 K [1]	$B_{ss,\ 4.2K}$	T	14.57	14.18
Short sample field, at 1.9 K [1]	$B_{ss,\ 1.9K}$	T	15.79	15.37
Temperature margin at 4.2 K at 13 T	$\Delta T_{B0=13T,\ 4.2K}$	K	2.03	1.61
Position on the load line at 4.2 K [2]	$\Delta B_{4.2K}$	%	89.2	91.7
Position on the load line at 1.9 K [2]	$\Delta B_{1.9K}$	%	82.3	84.6
Current for B_0 = 13 T	$I_{B0=13T}$	kA	13.1	13.4
Ratio peak field on coil over central field	λ	/	1.055	1.086
Magnetic field multipoles at 2/3 Φ_b	b_3	/	0.0	0.0
	b_5	/	0.0	0.0
	b_7	/	0.0	1.8
	b_9	/	0.1	-1.8
Stored magnetic energy per unit length at B_0	$E_{B0=13T}$	MJ/m	3.6	3.8
Inductance per unit length	L	mH/m	41.1	42.2
MECHANICAL PARAMETERS				
Lorentz forces per unit length [3]	F_X	MN/m	8.00	8.30
	F_Y	MN/m	-6.40	-6.31
Max compressive stress on conductor [4]	σ_c	MPa	130	122

Tab. 4.3.1. Quantitative comparison of cos-θ and block configuration without iron yoke

To compare approximately the conductor cost for both layouts, we can look for a block layout providing the same margin at 4.2 K as the baseline cos-θ configuration studied in § 4.1. This corresponds to an increase of 2.5% of the short sample field. The number of turns is no longer fixed. Keeping similar constraints, i.e., the first conductor on the lower blocks at a x = 60 mm, the top blocks at y = 55 mm, and b_3 and b_5 set to 0, it is found that a 44-44-44-44 block configuration is appropriate. This corresponds to an increase of conductor of about 13%.

On the base of these figures, it can be inferred that the cos-θ layout is more efficient on the magnetic level whereas the block layout is more efficient in terms of compressive stress. Further optimizations remain possible.

Comments:

[1] $B_{ss,\ 4.2\ K}$ ($B_{ss,\ 1.9\ K}$) is the short sample field at 4.2 K (1.9 K), i.e. the magnetic field attained in the centre of the dipole when the load line hits the critical surface of the cable. The critical surface integrates a 10% degradation due to cabling with respect to the virgin strand.

[2] relative position with the critical curve.

[3] per quadrant, without iron, B_0 = 13 T.

[4] stress values given on the base of the model assuming an impregnation in pairs (Fig. 4.1.6 and 4.2.7).

5. Qualitative comparison

The previous quantitative study has kept both layouts eligible for our purpose.

In this part, we intend to give the qualitative reasons that have made us favour the block design to go on with the detailed study. This chapter consists of a list of arguments that we consider strong enough to justify our decision.

5.1 Magnetic structure

The cos-θ structure seems to be mechanically limited in terms of the stress-management. Increasing pre-stresses are necessary to compensate for the increasing Lorentz forces, leading to very high cumulated stresses on the coil mid-plane, thus approaching critically the material limits.

Even if cos-θ designs can still be improved, we think that the evolution towards very high field accelerator magnets supposes to explore alternative solutions. The block layout is a promising candidate for this exploration, and has already been prospected at Berkeley. Solutions for the mechanical structure have been proposed, combining a thermal pre-stress provided by a shrinking shell around the structure with a variable pre-stress utilizing bladder and keys [18]. This solution, experienced by LARP on cos-θ as well as block layouts [19], has shown very good results even if some issues remain on the table.

At CERN, the subscale racetrack dipole magnet SMC is about to be tested in collaboration with RAL and CEA, using this structure principle with support from Berkeley [20]-[21]. This is a key step to get the know-how on this technology. We are confident that the EuCARD-HFM magnet structure will benefit from this experience.

For these reasons, we now consider that the time has come to apply the block layout technology to a real facility magnet, as EuCARD-HFM.

5.2 Ends shape

It has been considered that designing and winding the ends with the cos-θ layout would be possible in any case. This strong assumption is based on a wide experience of the involved labs, and on the fact that the specified cable (§ 1.3) is similar to existing ones. For instance the keystoned MSUT inner layer cable, from Twente, has a section of 1.97/2.21 mm x 21.8 mm with 33 strands [22]. We have made the decision not to perform an experimental in cos-θ configuration trial at this step.

On the contrary, the end geometry with the block layout raises the potential problem of the hard-way bending, when the cable is bent in its main plane, as shown on Fig. 5.2.1. Such a flared end design is necessary to have the requested aperture. In this region, the cable behaviour depends on its geometry and rigidity, and on the end shape itself. The experience of HD2 has shown that the question of the ends can have some issues [11].

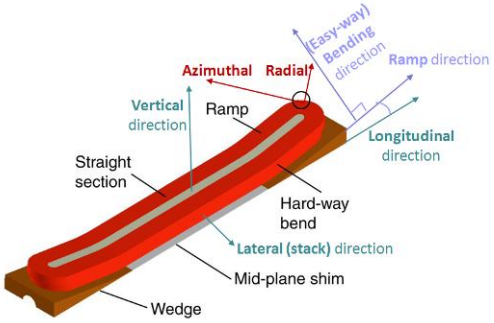

Fig. 5.2.1. Definition of the zones and axis of a flared racetrack (on the example of HD2)

To verify that such a coil design is feasible with our cable, a bending test has been performed, using a dedicated tooling (as shown on Fig. 5.2.2) with dummy copper bare cable [23]-[24].

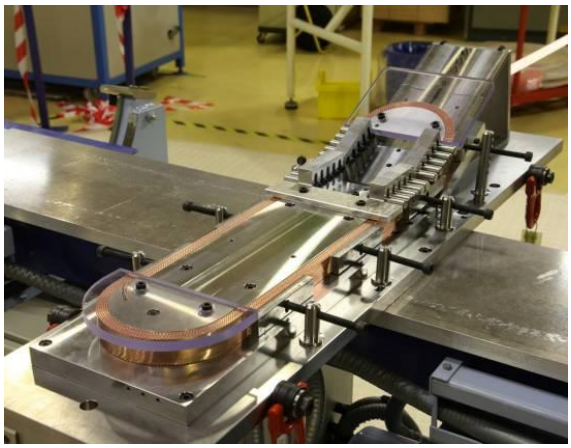

Fig. 5.2.2. Bending test tooling (final configuration)

A bending angle of 25°, considered as the largest reasonable value (and also the most critical in terms of bending radius), has been tested with ten turns. A practical aperture of 120 mm has been respected, as fixed in § 1.4. The winding tension has been set to 300 kN. The end was circular.

The flared configuration has been shown to be possible with this 25° angle. The cable used has remained stable and a good winding quality has been achieved, as shown on Fig. 5.2.3. No objection against the block design has been highlighted here. Additional tests with other parameters (lower angles, opposite winding direction) have confirmed this result.

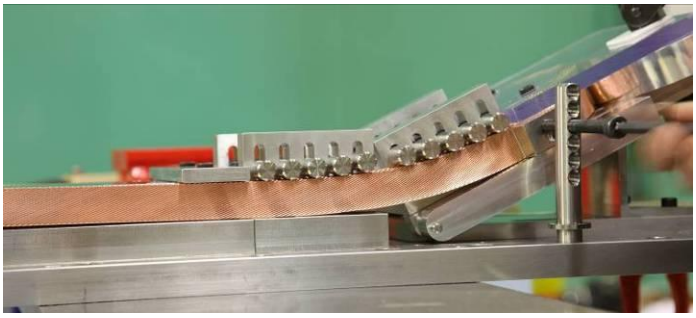

Fig. 5.2.3. Close-up on the hard-way bend zone after several turns

5.3 Electromagnetic aspects

For the EuCARD-HFM magnet, varying magnetic field is not an issue. Nevertheless, for accelerator application, the possibility of having varying field must be considered.

Cos-θ magnets have the broad face of their cable perpendicular to the magnetic flux, leading to large current loops and then to high AC losses. On the contrary, within the block structure, most of the conductors have their broad face parallel to the magnetic flux. This leads to lower losses.

5.4 Mechanical aspects

5.4.1 High stress zone location

The baseline analysis presented in §4 has not shown big difference in terms of absolute stresses between the layouts. Nevertheless, it can be inferred from Figs. 4.1.2, 4.1.6, 4.2.2 and 4.2.7 that with the cos-θ layout, the higher stress regions after energization will naturally occur along the magnet mid-plane, that includes high field regions close to the bore. The Lorentz forces in the block tend to push the magnet outwards. The high stress regions are away from the central high field region.

The block layout could be optimized in the high stress area so that to reduce or to displace the peak stress value. This is not possible with the cos-θ layout for which the high stress and the high field zones will always remain close.

5.4.2 Tolerances on the coil geometry

The finite element models typically assume perfect coil sizes and uniform mechanical properties. In the case of Nb-Ti magnets (with porous polyimide insulation and with polyimide pre-preg insulation) the azimuthal size and the elastic modulus are systematically measured to fine-tune the assembly parameters by shimming. The initial assembly parameters are defined by Finite Element Analysis and then often verified with an instrumented mechanical model. With a larger number of winding layers, the balancing of a set of parallel springs becomes more complex. The coils are manually wound and as such, even with best efforts their dimensions and elastic properties (spring constant) vary.

Due to the brittle nature of the Nb_3Sn coils, the measurement of the azimuthal size and the modulus in a similar way as in Nb-Ti coils is risky. The presently available measurement equipment are based on compressing the coil over a short length of some 100 to 150 mm, and therefore could not be used on Nb_3Sn coils other than at very low pressure, otherwise the shear stress would damage the reacted strands. The Nb_3Sn coils are presently vacuum-impregnated with resin under slight compression and the coil dimensions are defined by the mould cavity and hence the variations are expected to be small. The experience from LARP, however, is that the coil dimensions can vary up to 0.2 mm [25]-[26]. Additional difficulty with multilayer Nb_3Sn coils is that their Young modulus is typically three to four times higher than with Nb-Ti coils. Consequently, for the same displacement, the stress varies by the same factor making them more sensitive to the geometrical tolerances.

In this sense the block coil concept is expected to be easier to assemble, as in practice the four winding layers make up two parallel blocks. In addition, the material properties are uniform over the coil thickness and the pre-loading can be more easily controlled in the directions perpendicular and parallel to the conductor blocks. The difficulty of minimizing the bending stress, often significant in cos-θ magnets, can also be avoided with the block coil concept.

The coil fabrication tooling and the end spacers for the block coils are simpler and easier to manufacture that for the cos-θ coils. The number of end spacers will also be significantly smaller in a block configuration.

5.4.3 Stress management with block layout

The aim of this study is to decrease the stress in the third block (over 140 MPa) by keeping the field quality. The considered solution is so to add a shim in the upper blocks. Specified data are the following:

- Internal Radius ≥ 60 mm.
- Number of turns = 156 with a baseline configuration 41-41-37-37.

The optimization gives the following result for a central field of 13 T (here B_0=13.09T) [27]:

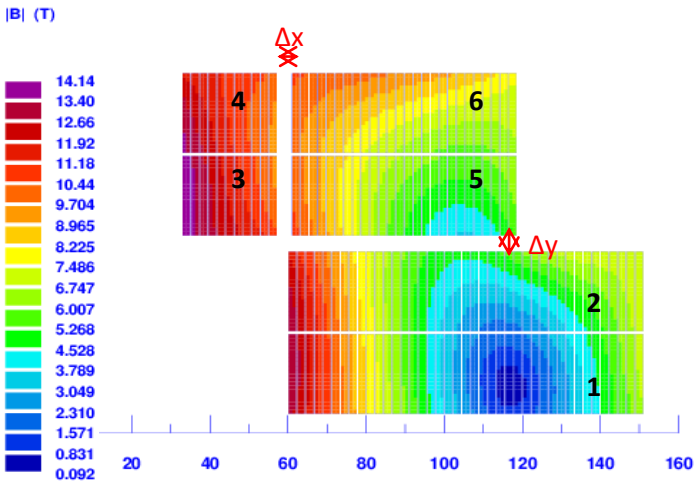

$B_{ss,\ 4.2\ K}$ = 14.31 T
$B_{ss,\ 1.9\ K}$ = 15.40 T

$I_{ss,\ 4.2\ K}$ = 14.6 kA

λ = 1.08

b_3 = 0.0
b_5 = 0.0
b_7 = 2.4
b_9 = -2.04

$E_{B0\ =\ 13\ T}$ = 3.81 MJ/m
L = 42.7 mH/m

Fig. 5.4.1. Magnetic field with a shim

A complete study gives the following results:

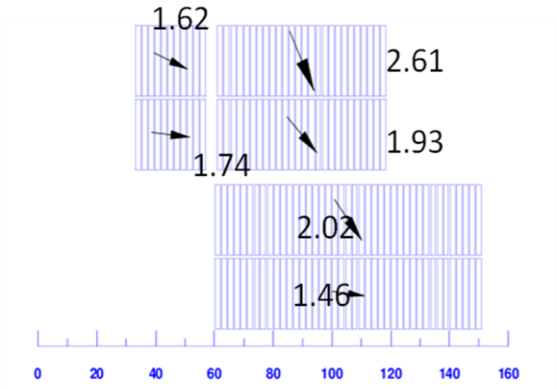

Fig. 5.4.2. Forces in the blocks with a configuration 41-41-37 (11+26) - 37 (11+26).
The values indicate the magnitudes of the forces in MN/m.

Block number	1	2	3	4	5	6
Horizontal force F_X [MN/m]	1.45	1.21	1.73	1.49	1.33	1.09
Mean horizontal stress [MPa]	66	55	79	68	61	50
Vertical force F_Y [MN/m]	-0.17	-1.62	-0.19	-0.65	-1.41	-2.37
Mean vertical stress [MPa]	-2	-18	-8	-27	-24	-41

Tab. 5.4.3. Forces and stresses in the blocks

As a conclusion, the upper block can be subdivided with shims in order to reduce the Lorentz forces without degrading the field quality, provided the shim thickness remains under 4 mm. This study makes sense only if it is verified that this thickness is sufficient to maintain the stresses, and if it is possible to provide the pre-stress at this location.

5.5 Practical aspects

5.5.1 Realization

As explained in § 5.4, the pre-stress is easier to apply with the block design, because it is mostly parallel to the cable stacking direction. In this configuration, the mechanical efforts are transmitted via flat surfaces, limiting local peaks. Moreover, the block layout does not suffer from radial size problems during heat treatment: the conductor inflation can be more easily controlled. On the base of the bending test presented in § 5.2, the block winding is not complicated, even with flared ends. Thus, the tooling geometry is going to be simpler than with the cos-θ, as well for the winding as for the reaction and impregnation.

In addition it has been said that the tolerances can be controlled and adjusted more easily with the block layout, while playing mostly with planar shims. The possibility to play with the pre-stress shims gives more testing flexibility to the block configuration. However, the initial dimension of the coils must be controlled finely to insure the acceptable field quality, but this remains true for both layouts. Those considerations (tooling simplicity + relaxed tolerances on it) could lead to significant cost reductions. Most of all, they allow us to adjust our tooling once the parts have been fabricated.

A major practical argument in favour of the block layout is that it allows a step-by-step approach: the double-pancakes can be built successively and tested individually. In the same way, replacing a damaged coil is far easier in this case.

5.5.2 Cost

The cost of the conductor in the magnet is higher with the block layout for fixed magnetic performances (+ 13%, cf. § 4.3). Nevertheless, the deliverable of the project is a one-off, and so the conductor represents a small fraction of the cost, which is driven by the development. Due to the simpler tooling envisaged and the smaller complications expected we could expect lower fabrication costs in the case of the block layout.

6. Conclusion

Within the EuCARD-HFM framework, the Magnet Pre-Design Working Group has compared candidate magnetic configurations for a 13 T Nb_3Sn dipole with a 100 mm aperture.

The comparative study has been focused from the beginning on two magnetic layouts: the cos-θ and the block. Other solutions such as hybrid or graded magnets have been considered too risky due to our time and resources constraints.

The baseline analytic comparison has shown no fundamental difference likely to discard any of these layouts. The feasibility to wind flared ends with our cable in the block configuration has been verified experimentally.

Knowing our constraints, a certain number of qualitative considerations lead us to favour the block solution. In particular:

- the need to explore new solutions for future accelerator magnet application (the EuCARD-HFM magnet must be considered as a first step toward innovative magnet structures);

- the greater simplicity and versatility of the tooling and the testing procedure;

- the fruitful experience from LARP;

- the on-going development program on the SMC.

Since no objection has been identified against this solution, we consider that we can go on with the block layout for the detailed study.

Acknowledgement

The MPWG wish to acknowledge every people who participated in this study, in particular: Jean-François Millot for the detailed conception of the test tooling, Alain Przybylski and Jean-Jacques Goc for the bending test, Alain Porcher, Aubrey Poulizac and Thomas Dalla-Foglia for their assistance.

We would also like to thank all the EuCARD project members and Shlomo Caspi at Berkeley for the interesting discussions we have had with them.

The research leading to these results has received funding from the European Commission under the FP7 Research Infrastructures project EuCARD, grant agreement n° 227579.

This work is part of EuCARD Work Package 7: Super-conducting High Field Magnets for higher luminosities and energies.

Tables and figures

References

[1] EuCARD-HFM public website, http://eucard.web.cern.ch/eucard/activities/research/WP7

[2] Overview and status of the Next European Dipole (NED) joint research activity, A. Devred et al., Supercond. Science Technol., vol. 19, 2006.

[3] FRESCA2 magnet specification, G. de Rijk with SWG

[4] EuCARD project contractual requirements

[5] S. Russenschuck, Field Computation for Accelerator Magnets: Analytical and Numerical Methods for Electromagnetic Design and Optimization. Wiley-VCH, first edition, March 2010

[6] Electromagnetic design of superconducting dipoles based on sector coils, L. Rossi and E. Todesco, Phys. Rev. special topics – Accelerators and beams, 10, 112401 (2007)

[7] Electromagnetic efficiency of block design in superconducting dipoles, L. Rossi and E. Todesco, IEEE Trans. Appl. Supercond. 19 , 3 (2009), p. 1186-1190

[8] Design and fabrication of end spacers for a 13 T Nb3Sn magnet, S. Caspi, D. Dell'Orco, W.B. Ghiorso, A. Wandesforde, IEEE Trans. Appl. Supercond. 5 , 2 (1995), p. 1004-1007

[9] Test results for a high field (13 T) Nb3Sn dipole, A.D. McInturff, R. Benjegerdes, P. Bish, S. Caspi, K. Chow, D. Dell'Orco, D. Dietderich, R. Hannaford, W. Harnden, H. Higley, A. Lietzke, L. Morrison, M. Morrison, R. Scanlan, J. Smithwick, C.Taylor, J. van Oort, PAC-97, Vancouver, May 1997

[10] Fabrication and Component Testing Results for a Nb3Sn Dipole Magnet, D. Dell'Orco et al., IEEE Trans. Appl. Super. 5 (2), June 1995, p. 1000-1003

[11] Recent test results of the high field Nb3Sn dipole magnet HD2, P. Ferracin, B. Bingham, S. Caspi, D.W. Cheng, D.R. Dietderich, H. Felice, A.R. Hafalia, C.R. Hannaford, J. Joseph, A.F. Lietzke, J. Lizarazo, G. Sabbi, and X. Wang, MT21, Heifei, China, 2009

[12] P. Ferracin, private communication

[13] Task 4: HTS dipole insert conceptual design, M. Bruchon, M. Durante, T. Lécrevisse, J.-M. Gheller, O. Louchart, J.-M. Rey. Presented by J.-M. Rey during the Wroclaw EuCARD meeting, March 2010

[14] ANSYS 11.0 Documentation

[15] Mechanical Properties for NED SMC Computations, P. Loveridge, F. Regis, P. Manil, Oct. 2007, EDMS 683000 V5.2

[16] LHC design report, Vol. I, The LHC main ring, O. Brüning et al., 2004

[17] Presented by A. Milanese during the Wroclaw EuCARD meeting, March 2010

[18] The use of pressurized bladders for stress control of superconducting magnets, S. Caspi, IEEE Trans. Applied Superconductivity, vol. 16, Part 2, pp. 358–361, June 2006.

[19] LARP public website, http://larp.fnal.gov

[20] Magnetic design and code benchmarking of the SMC (Short Model Coil) dipole magnet, P. Manil, et al., IEEE Trans. Applied Superconductivity, to be published.

[21] Mechanical design of the SMC (Short Model Coil) dipole magnet, F. Regis, et al., IEEE Trans. Applied Superconductivity, to be published.

[22] An Experimental 11.5 T Nb3Sn LHC Type of Dipole Magnet; A. den Ouden, S. Wessel, E. Krooshoop, R. Dubbeldam and H.H.J. ten Kate, Appl. Supercond. 30 , 4 (1994), p. 2320

[23] Rapport sur les essais de cintrage des têtes de bobine, F. Rondeaux, A. Przybylski, P. Manil, CEA note n°SAFIRS-00152-A, May 2010

[24] CERN visit report, A. Milanese, April 2010

[25] LQS01 Mechanical Analysis and LQS01b Assembly, P. Ferracin, presented at the LARP Collaboration Meeting 14, April 2010

[26] HQ Progress and Plan, H. Félice, presented at the LARP Collaboration Meeting 14, April 2010

[27] Influence of a shim on the field quality, M. Bruchon, CEA report, May 2010